

Heterogeneity of hydraulic conductivity and Darcian flux in the submerged streambed and adjacent exposed stream bank of the Beiluo River, northwest China

Jinxi Song^{1,2} · Weiwei Jiang² · Shaofeng Xu² · Guotao Zhang² · Liping Wang² · Min Wen² · Bo Zhang² · Yuanyuan Wang² · Yongqing Long²

Received: 19 January 2016 / Accepted: 8 July 2016 / Published online: 10 August 2016
© Springer-Verlag Berlin Heidelberg 2016

Abstract Recognizing the heterogeneity of hydraulic conductivity and hyporheic flow is critical for understanding contaminant transfer and biogeochemical and hydrological processes involving streams and aquifers. In this study, the heterogeneity of hydraulic conductivity and Darcian flux in a submerged streambed and its adjacent exposed stream banks were investigated in the Beiluo River, northwest China. In the submerged streambed, Darcian flux was estimated by measurement of vertical hydraulic conductivity (K_v) and vertical head gradient (VHG) using in-situ permeameter tests. On exposed stream banks, both horizontal hydraulic conductivity (K_h) and K_v were measured by on-site permeameter tests. In the submerged streambed, K_v values gradually decreased with depth and the higher values were concentrated in the center and close to the erosional bank. Compared to the exposed stream banks, the K_v values were higher in the streambed. From stream stage to the topmost layer of tested sediment, through increasing elevation, the K_h values increased on the erosional bank, while they decreased on the depositional bank. The values of VHG along the thalweg illustrate that downwelling flux occurred in the deepest area while upwelling flux appeared in the other areas, which might result from the change of streambed elevation. The higher value of the Darcian flux in the submerged streambed existed near the erosional bank.

Keywords Hydraulic properties · Vertical head gradient · Streambed · Groundwater/surface-water relations · China

Introduction

Quantifying the magnitude and spatial distribution of hydraulic conductivity (K) in both a streambed and its associated stream bank is not only significant for determining hyporheic water exchange, but also plays an important role in understanding a number of hydrogeological problems (Conant 2004; Song et al. 2009; Levy et al. 2011; Dong et al. 2012; Chen et al. 2014). It is known that both vertical hydraulic conductivity (K_v) and horizontal hydraulic conductivity (K_h) of a streambed usually have heterogeneity at measured scale (meters to hundreds of meters) or large catchment scale (hundreds of kilometers; Chen 2004; Leek et al. 2009; Min et al. 2013; Xi et al. 2015). The spatial variations of streambed hydraulic conductivity (K_v , K_h) and anisotropy have been analyzed and documented by many researchers (Chen 2004; Song et al. 2007; Min et al. 2013; Sebok et al. 2015). Streambed K_v is highly variable in space; the greatest K_v generally being observed in the center of the channel (Genereux et al. 2008). Streambed K_v and K_h generally decreases with increasing depth within 1 m (Ryan and Boufadel 2007; Song et al. 2007; Wu et al. 2016), whereas streambed anisotropic ratios (K_h/K_v) close to stream banks can span four orders of magnitude (Sebok et al. 2015). Several researchers have concentrated their work on exposed sediment hydraulic conductivities such as are present in point bars (Dong et al. 2012), in cross bedding in fluvial sediments (Cheng et al. 2013), and in a high floodplain (Chen et al. 2014); however, the accurate quantification and characterization of

✉ Jinxi Song
jinxisong@nwu.edu.cn

¹ State Key Laboratory of Soil Erosion and Dryland Farming on the Loess Plateau, Institute of Soil and Water Conservation, CAS & MWR, Yangling 712100, China

² College of Urban and Environmental Sciences, Northwest University, Xi'an 710027, China

hydraulic conductivity in streambeds and their associated stream banks remains a challenging task because of problems related to field conditions and measurement scales (Min et al. 2013), and complexity of the heterogeneity and anisotropy (Anibas et al. 2011).

Heterogeneity of the hydraulic conductivity and that of hydraulic exchange has an interrelationship; determination of the heterogeneity pattern of hydraulic conductivity and its response mechanism to hydraulic exchange is of great importance in understanding stream–aquifer interactions (Cardenas et al. 2004; Sawyer and Cardenas 2009; Koch et al. 2011; Pryshlak et al. 2015). Long hyporheic exchange paths can be produced where there is permeability heterogeneity (Sawyer and Cardenas 2009). Modeling studies indicated that minimum discharges of observed and simulated hydrographs were sensitive to hydraulic conductivity (Koch et al. 2011). Upward flow in streambeds mechanically increases sediment pore size, which can result in increased streambed K (Song et al. 2007; Dong et al. 2012). Chen (2011) confirmed that fine sediments carried by hyporheic water could travel several meters altering K_v distribution with depth. In losing stream reaches, K_v increases with the depth to 10 m in an aquifer, in contrast to gaining stream reaches where the distribution pattern of K_v is the opposite (Chen et al. 2013). Low-permeability sediment layers can cause great changes in the intensity of hyporheic exchange and the shape of the hyporheic zone both under neutral and upwelling conditions (Gomez-Velez et al. 2014). K heterogeneity increases interfacial fluxes, changes the shape of residence time distributions, and decreases median residence times (Pryshlak et al. 2015).

In addition to being affected by the heterogeneity of hydraulic conductivity, hyporheic exchanges can be dominated by variable pressure heads in their streambed sediments and the surrounding features (Cardenas et al. 2004; Koch et al. 2011). Stream geomorphology attributes have been recognized as controlling factors in the behavior of regional hydraulic interaction in stream–aquifer systems (Boano et al. 2006; Cardenas 2009; Sebok et al. 2015). The variable pressure heads are always created by stream geomorphology, including bedforms (Sawyer and Cardenas 2009), meanders (Sebok et al. 2015), riffles and pools (Käser et al. 2009; Hatch et al. 2010), sinuosity (Boano et al. 2006; Cardenas 2009), cobbles and beaver dams (Genereux et al. 2008), point bars (Dong et al. 2012) and channel gradient (Cardenas et al. 2004). Streambed features are more variable in the meanders than in the straight channel because of the more dynamic environment in the meanders (Sebok et al. 2015). Downward and upward flow paths can be induced by bedforms and sinuosity at the meter scale (Malard et al. 2002). Additionally,

topographical factors including the slope, width, elevation and length of the channel together can influence the streambed K (Xi et al. 2015). The interaction of surface water and groundwater can be intensified by the growth of meander length and weakened by a decrease in river sinuosity (Boano et al. 2006; Cardenas 2009).

An anabranching channel is one of the important sedimentological forms that connect regional aquifers and streams (Huang and Nanson 2007). Water can be diverted from the main channel into slower moving pools by anabranches, facilitating infiltration into the subsurface (Koch et al. 2011). In addition, a stream bank is a major part of a fluvial system that represents an important depositional environment (Chen et al. 2014) and influences groundwater/surface-water interaction with the connected aquifer (Batlle-Aguilar et al. 2015). An increase in hydraulic conductivity with increasing elevation of the stream bank was found to induce low recharge rates (2–5 cm/year) and long residence times (years to decades) of groundwater recharge (Böhlke et al. 2007). 2.5 orders of magnitude differences of net streambed fluxes were found to occur between a streambed and its adjacent stream bank (Shope et al. 2012). The stream and aquifer become laterally connected through a high-permeability preferential path in the stream bank even though groundwater heads were all below the streambed (Batlle-Aguilar et al. 2015). The effect of aquifer anisotropic K ratios on modeling stream flow depletion is very striking; the error of analytical solution will be larger for a strong anisotropic aquifer (Chen and Yin 1999). Generally, the sediments in a streambed are coarser than that in its stream bank, which leads to different ranges and statistical features of hydraulic conductivity in the streambed and in the stream bank (Chen et al. 2014). A wide range of sandy-loam to clay-loam sediments was found between the streambed and stream banks (Batlle-Aguilar et al. 2015). It is, therefore, necessary to determine the heterogeneity of sediment K in an integrative river channel combined with the streambed and its stream bank, which is of great help in more appropriate modeling approaches for stream–aquifer interactions; however, only a few studies have investigated the heterogeneity of K_v and K_h in both a streambed and its associated stream banks. The aim of this research was to get a better understanding of such variability of hydraulic conductivity and Darcian flux by way of a case study in both a streambed and its adjacent stream bank.

In the present study, K_v and vertical head gradient (VHG) were determined by applying an in-situ permeameter test to estimate Darcian flux in a 100-m-long section in an anabranching channel. In addition, on-site permeameter tests were used to obtain the K_h and anisotropy on both the erosional bank and depositional bank of the studied stretch. Specific objectives of this study were to (1) determine the spatial

distribution of streambed K_v , VHG, and Darcian flux; (2) investigate the heterogeneity of K_h and anisotropy of both its associated stream banks; and (3) relate this variability of VHG and Darcian flux to stream geomorphology, bedform, sediment grain size and temperature.

Study area

This study was performed in the Beiluo River, situated in Shaanxi Province, China, which is not only the longest tributary of the Weihe River, but also a meandering stream (Fig. 1).

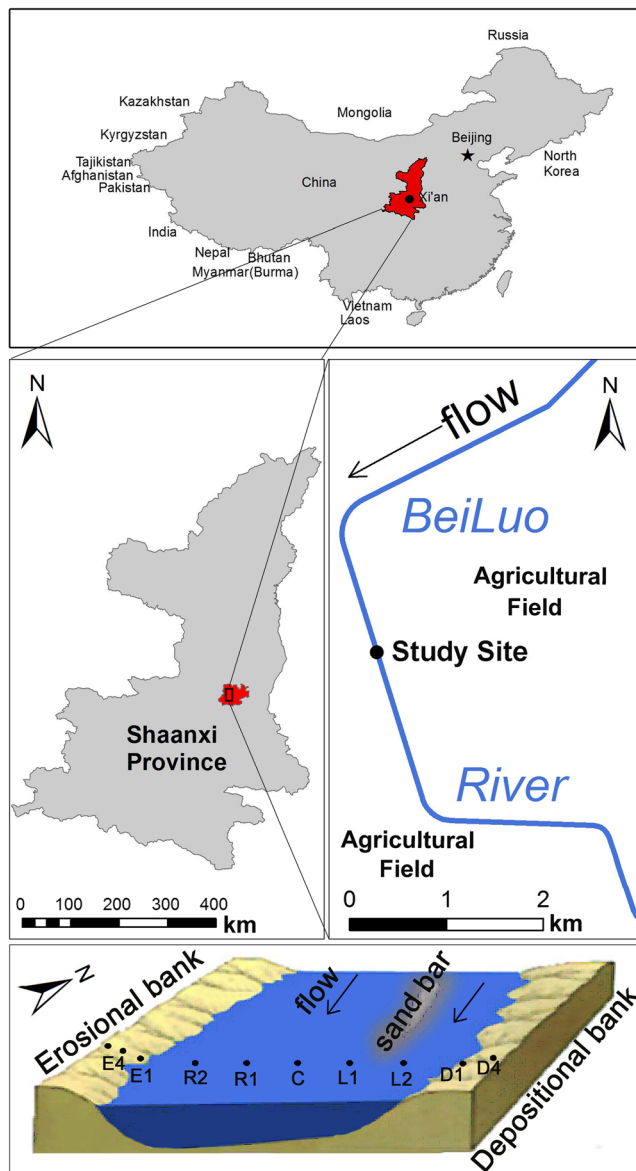


Fig. 1 The location of the study site (R2, R1, C, L1 and L2 indicate right side, right side to center, center, left side to center, and left side of submerged streambed, respectively). E1, E4, D1 and D4 indicate the locations for anisotropy (K_v/K_h) tests on both exposed banks

The study area is located in the transition region from the Loess Plateau to the Guanzhong Basin. The river system has a stream slope of 1.98 ‰ with an average stream flow of 14.99 m³/s.

A field site suitable for in-situ testing was chosen to study spatial variability and relations between streambed K_v , Darcian flux, stream geomorphology and bedforms in the streambed (Fig. 2), and heterogeneity and anisotropy on both associated stream banks (Fig. 3). In this study, the test locations were conducted at 100-m scale along the stream flow, starting from 10 m downstream of anabranching channels in January 2015 (Fig. 1) when the highest velocity and average water depth were <1.0 m/s and 1 m (Fig. 2), respectively. Due to the difference in streambed topography, suspended sediment likely settles out near the bank where streambed elevation is higher and flow velocity is lower. This bank can be called the depositional bank, while the opposite bank is likely incised by stream flow and the materials can be washed away downstream; the opposite bank can be termed erosional bank (Fig. 2). The downstream section of the anabranching river was divided into two sub-branches by a 13-m-long sand bar. Along the flow direction, the sediment on the right stream bank is being eroded, while depositional processes occur at the left bank (Fig. 1). The average channel width was 35 m. Field measurements in the streambed were made over five transects, each with five test locations, forming a measurement grid (Fig. 2). In total, 25 measurements of K_v and VHG values were obtained. It can be hypothesized that the composition of sediment particles may be significantly different for each test location. Based on field investigation, the streambed sediment differs significantly with depth. The surface streambed sediment, at depths less than 30 cm, generally is composed of sand and, deeper than 45 cm, it mostly consists of silt and clay. Sediments between 30 and 45 cm depth are a mixture, differing from the other two in that they contain all three components, sand, silt and clay. Consequently, the heterogeneity of K_v as a function of depth in the three connected layers was also determined (Table 1).

The local erosional and depositional processes have resulted in steep banks at the field site; the erosional bank and depositional bank were an average of 5.6 and 3.2 m above the stream stage at the time of measurement, respectively (Fig. 3). The sediment composition and sedimentary structures of both stream banks were investigated. Three test layers on the erosional bank and two test layers on the depositional bank were identified by elevation to stream stage and their sedimentary structure and composition (Table 2). K_h measurements for each layer of the banks were made along the flow direction at seven test points. Additionally, a total of 12 groups

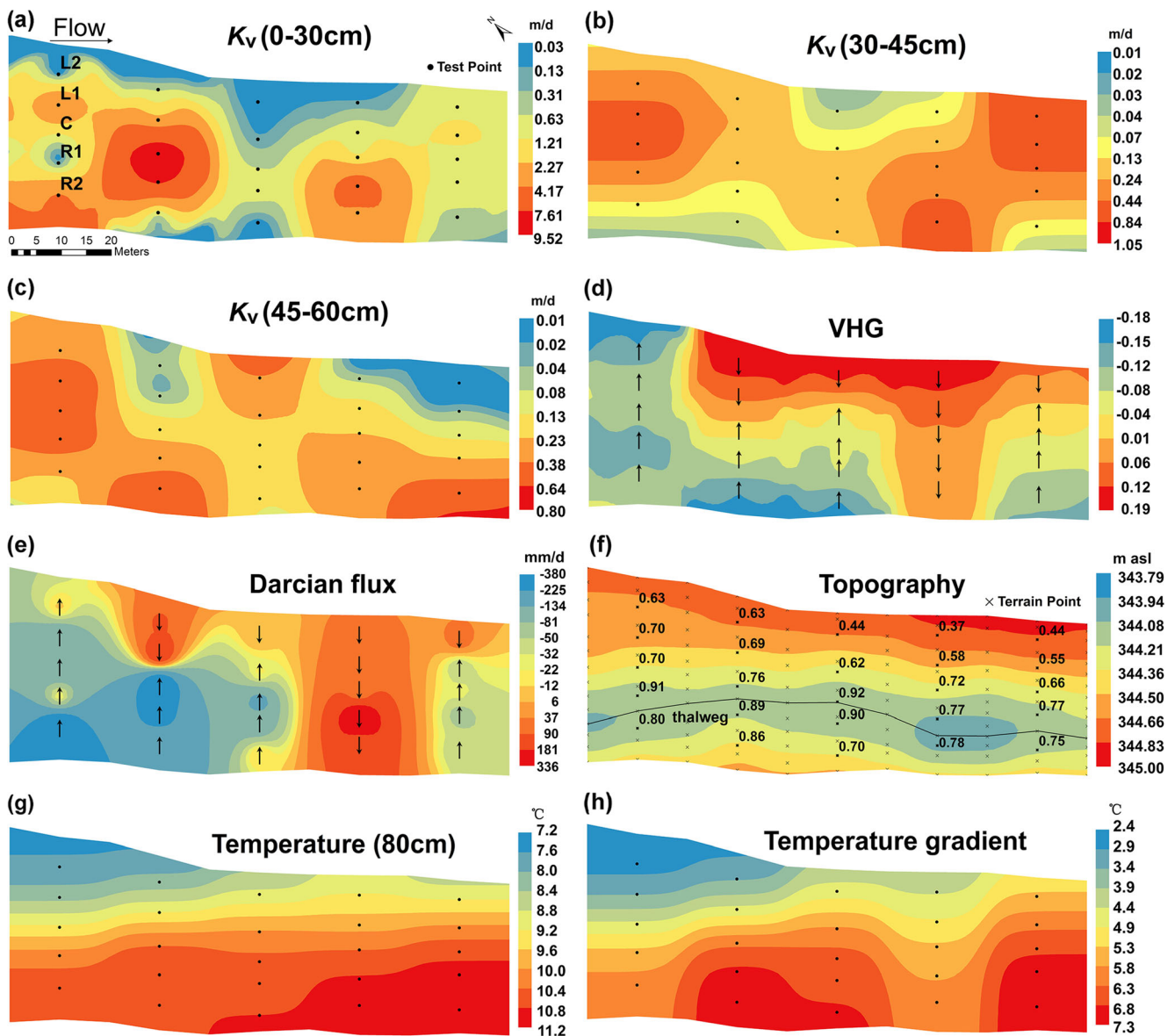


Fig. 2 Interpolated contour maps of K_v for **a** upper layer, **b** middle layer and **c** lower layer from a birds-eye view (*R2*, *R1*, *C*, *L1* and *L2* indicate right side, right side to center, center, left side to center and left side of submerged streambed, respectively), **d** VHG (arrows pointing toward the top of the page indicate upwelling flux), **e** Darcian flux (derived from K_v

for upper layer), **f** topography (m asl, streambed elevation in meters above sea level; number given at each site indicates the velocity in m/s), **g** temperature at the depth of 80 cm in the streambed, and **h** temperature gradient (temperature difference with comparison of 0 to 80 cm of streambed sediment)

of sediment samples were chosen for determining the anisotropy of both banks (Fig. 3).

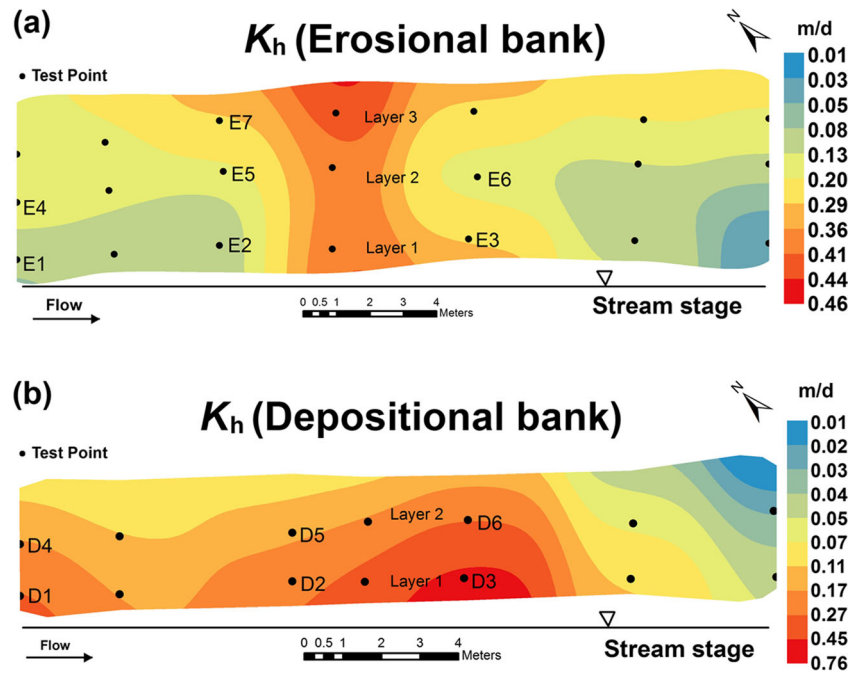
Methods

Streambed K_v tests at different depths for three connected layers

In this study, an in-situ permeameter test, as describe by many researchers (Chen 2004; Genereux et al. 2008; Dong et al.

2012; Min et al. 2013), was used to determine the streambed K_v in three connected beds. The procedure includes three steps: first, polyvinyl chloride (PVC) pipe with an inner diameter of 5.4 cm and length 160 cm was used. The pipe was vertically inserted into the streambed upper layer, ensuring that the length of the sediment column was approximately 30 cm (*L1*, Fig. 4a). During the test, water was added from the top (open) end of the pipe to create a hydraulic head. The head was then allowed to fall in the pipe. For each permeameter test, during the water-level decline (inside the pipe), hydraulic head measurements were collected at a given

Fig. 3 Interpolated contour maps of K_h on the **a** erosional bank and **b** depositional bank from a cross-sectional view. The letters on the diagrams indicate the locations for anisotropy (K_v/K_h) tests on both banks



time interval. Second, after the upper-layer test, the permeameter was pressed deeper into the sediment, thus making sure that the length of the sediment column was about 45 cm (L_{1-2} , Fig. 4a). The aforementioned test method was then repeated in the 0–45 cm depth interval. Third, the same procedure was repeated for the third layer with a depth interval of 0–60 cm (L_{1-3} , Fig. 4a). K_v values can be calculated using the following equation proposed by Hvorslev (1951):

$$K_v = \frac{\pi D}{t_2 - t_1} + L_v \ln(h_1/h_2) \tag{1}$$

where D is the inner diameter of the pipe, m is the square root of the ratio of the horizontal conductivity K_h to the vertical conductivity K_v (i.e., $m = \sqrt{K_h/K_v}$), L_v is the length of the sediment column, and h_1 and h_2 are the hydraulic heads inside the pipe measured at times t_1 and t_2 , respectively. Generally, K_h is larger than K_v . When $1 < m < 5$, if the ratio (L_v/D) is larger than 5, the modified Hvorslev solution can be simplified

to Eq. (2), and the error of the modified calculation will be less than 5% (Chen 2004). In this study, the average lengths of the sediment column were 30.3, 45.9 and 60.8 cm for L_1 , L_{1-2} and L_{1-3} , respectively. The inner diameter of the sediment column was 5.4 cm, so the ratio L_v/D was larger than 5, ensuring a relatively small error using these measurements.

$$K_v = \frac{L_v}{t_2 - t_1} \ln(h_1/h_2) \tag{2}$$

Additionally, the K_v of the middle layer (L_2) and lower layer (L_3) can be calculated using the following equations (Song et al. 2007).

$$K_{v2} = L_2 / (L_{1-2} / K_{v1-2} - L_1 / K_{v1}) \tag{3}$$

$$K_{v3} = L_3 / (L_{1-3} / K_{v1-3} - L_{1-2} / K_{v1-2}) \tag{4}$$

where K_{v1} , K_{v1-2} and K_{v1-3} are the corresponding vertical hydraulic conductivities for sediment column L_1 (0–30 cm),

Table 1 Statistical distribution of K_v values from permeameter tests in the submerged streambed

Layer	Number of samples	Range (m/d)	Mean (m/d)	Median (m/d)	Standard deviation	Standard error mean	Coefficient of variation	Normal distribution test
Upper layer	25	0.03–9.52	2.17	1.11	2.54	0.51	1.17	0.149*
Middle layer	25	0.01–1.05	0.28	0.14	0.31	0.06	1.11	0.125*
Lower layer	25	0.01–0.80	0.23	0.08	0.28	0.06	1.21	0.079*
Total	75	0.01–9.52	0.83	0.23	1.67	0.97	2.01	0.001

* Significance at 95 % confidence level

Table 2 Statistical analysis of the K_h values, sedimentary characteristics and anisotropy for each layer on both exposed stream banks

Parameter	Statistic	Erosional bank			Depositional bank	
		Layer 1	Layer 2	Layer 3	Layer 1	Layer 2
Average distance to stream stage (m)	–	0.7	3.2	4.8	0.5	2.0
Number of samples	–	7	7	7	7	7
K_h tests	Range (m/d)	0.03–0.42	0.01–0.37	0.17–0.42	0.06–0.76	0.02–0.05
	Mean (m/d)	0.17	0.11	0.31	0.34	0.04
	Standard deviation	0.16	0.13	0.10	0.24	0.01
	Coefficient of variation	0.94	1.18	0.32	0.71	0.25
	Normal distribution test	0.470*	0.742*	1.000*	0.989*	0.556*
Sediment description and grain size analysis	Sediment sample location for grain size analysis	E2	E5	E7	D2	D5
	Average thickness of measured sediment (cm)	35.5	41.2	34.3	38.2	33.0
	Sediment composition	Silt and clay	Fine sand and silt	Homogeneous silt with microlamination	Mixture of sand, silt and clay	Silt and clay
	<0.075 mm (silt+clay) %	81.1	75.4	89.8	35.1	78.4
	Average median grain size (mm)	0.041	0.054	0.037	0.094	0.048
Anisotropy measurements	coefficient of uniformity	1.9	2.5	1.3	5.2	2.5
	sediment sample location	E1, E2, E3	E4, E5, E6	–	D1, D2, D3	D4, D5, D6
	K_h/K_v ratio	2.6, 2.3, 0.7	2.5, 1.5, 2.3	–	1.5, 6.0, 3.3	3.8, 2.2, 0.9

* Significance at 95 % confidence level

L_{1-2} (0–45 cm) and L_{1-3} (0–60 cm); K_{v1} , K_{v2} and K_{v3} are the calculated vertical hydraulic conductivity for sediment column L_1 (upper layer, 0–30 cm), L_2 (middle layer, 30–45 cm) and L_3 (lower layer, 45–60 cm; Fig. 4a).

Vertical hydraulic gradient and estimation of Darcian flux

The hyporheic zone is an active ecotone of mixing between stream water and groundwater (Boulton et al. 1998). It is

difficult to determine the boundaries of hyporheic zone because they vary in time and space (Brunke and Gonser 1997; Boulton et al. 1998). Research has focused on the tens of centimeters to the depth of the hyporheic zone (Schmidt et al. 2007; Chen et al. 2009; Kennedy et al. 2010; Anibas et al. 2011; Gariglio et al. 2013). In the stream reach of this study area, the estimated depth of the hyporheic zone was estimated to be 30 cm. On the basis of measurement of vertical hydraulic gradient and vertical hydraulic conductivity by an in-situ pipe permeameter test, the Darcian flux pattern of upwelling or downwelling can be well

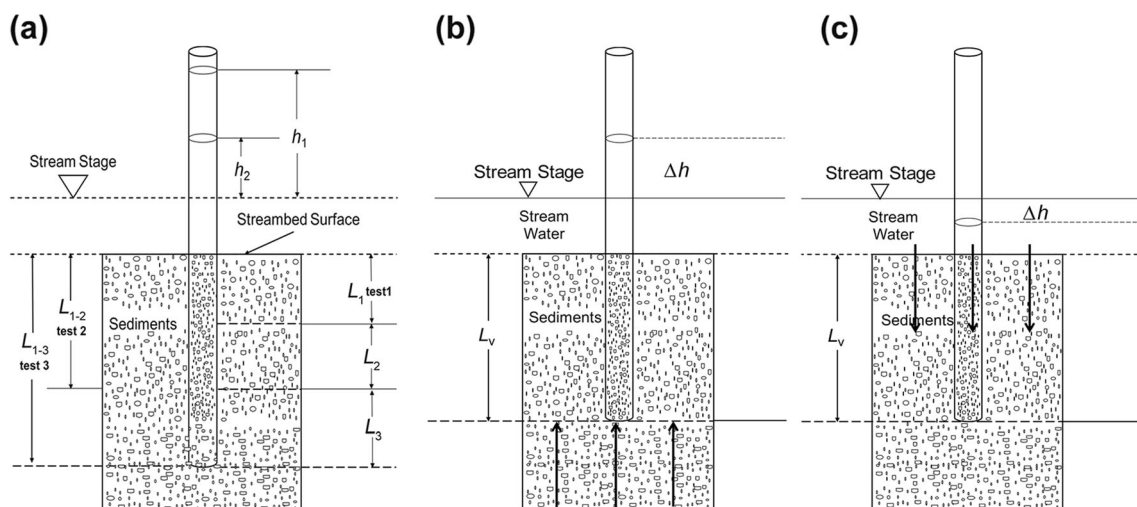


Fig. 4 Schematic diagram showing an in-situ permeameter test for determination of **a** streambed K_v with three connected sediment layers, and vertical head gradient measurements for **b** upwelling flow and **c** downwelling flow

illustrated. Before the K_v test, the pipe was left installed in the upper sediment layer for more than 16 h to test VHG. VHG values at each test point were calculated using the methods of Freeze and Cherry (1979):

$$i = \frac{\Delta h}{L_v} \quad (5)$$

$$q_v = i \times K_v \quad (6)$$

Where Δh is the hydraulic head difference measured from water level in the pipe and stream water level, L_v is the length of the sediment core in the pipe; i is the value of vertical hydraulic gradient, and positive values reflect inflow to groundwater (Fig. 4b,c). The Darcian flux (q_v), that is, the specific discharge, can be calculated using Darcy's law (Käser et al. 2009; Sebok et al. 2015).

Sediment coring and measurement of both stream banks

The heterogeneity and anisotropy of hydraulic conductivity were determined on both stream banks. On-site permeameter tests were performed to determine K of the exposed sediment following the method of Chen et al. (2014). The uncompacted surface sediment of the streambank was first scraped off, and then PVC pipe was hammered into the stream bank in the horizontal and vertical directions. The length of the sampling sediment columns for both directions was approximately 35 cm. The top opening of the pipe was sealed using a rubber cap to separate the pipe from the atmosphere, then the compact sediment column in the pipe was pulled out (Fig. 5a). Several layers of plastic screen were used to prevent the sediments from exiting the lower end of the pipe. After sediment cores were obtained, saturation tests for all sediment columns were performed using stream water and a bucket. River water was put into the bucket and its water depth was higher than the length of the core in the pipe. The pipe was kept vertical in the bucket for a while to make its saturation. During the process, water was absorbed by the sediment core from the lower end through the screen layers. The air in the sediment was forced to escape upward through the upper end of the core. After the saturation process was complete, the pipe was oriented vertically, using a tripod, and measurements of the hydraulic conductivity were begun using the in-situ method described in the preceding (Fig. 5b). The hydraulic conductivity for horizontal and vertical directions can be calculated from Chen (2004):

$$K_h = \frac{L_h}{t_2 - t_1} \ln(h_1/h_2) \quad (7)$$

$$K_v = \frac{L_v}{t_2 - t_1} \ln(h_1/h_2) \quad (8)$$

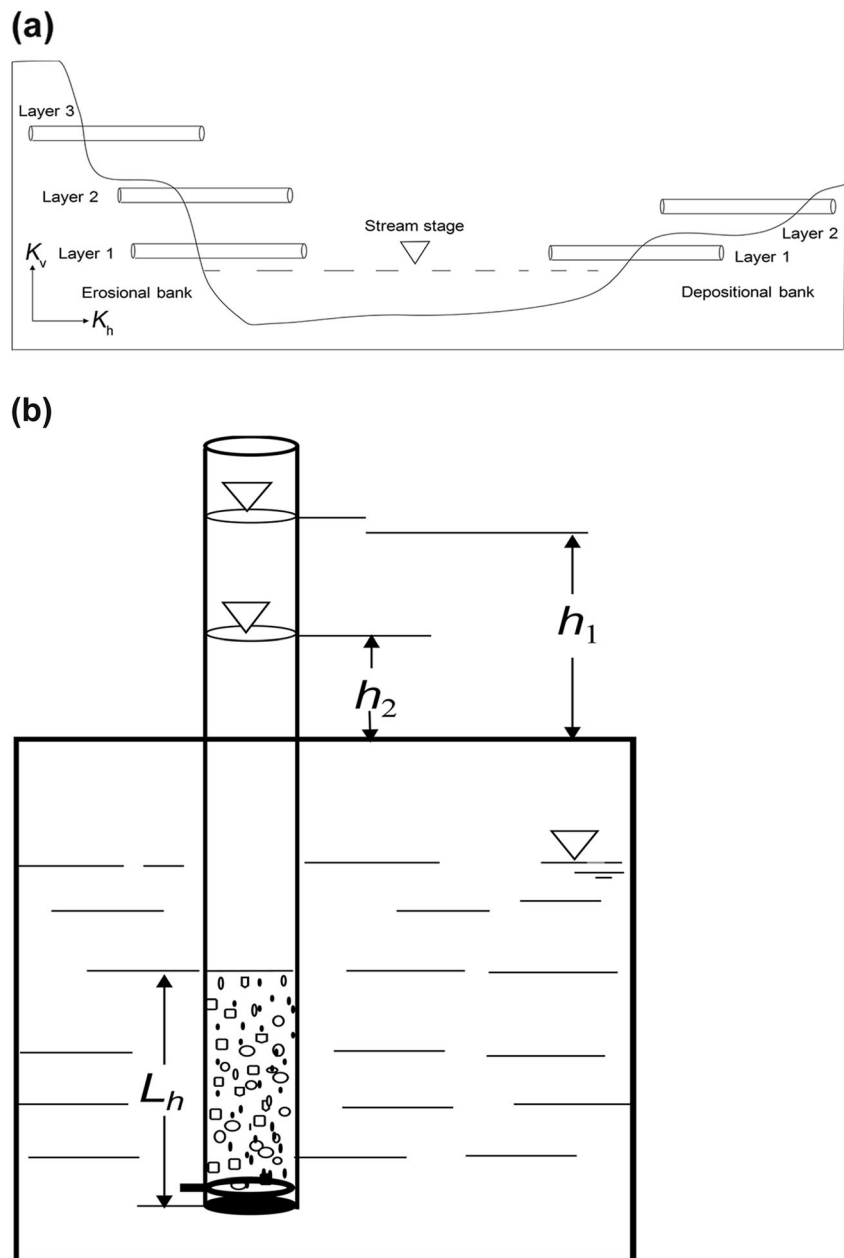
where L_h and L_v are the length of the sediment core in the pipe in the horizontal and vertical directions, respectively and h_1

and h_2 are the hydraulic head inside the pipe measured at times t_1 and t_2 , respectively.

Determination of various environmental variables

Numerous variables may contribute to streambed K and Darcian flux. These include water depth, flow velocity, erosional and depositional processes (Genereux et al. 2008), clogging sediment (Datry et al. 2015), bedforms (Cardenas et al. 2004), stream geomorphology (Sebok et al. 2015), sediment temperature (Hatch et al. 2010), hyporheic processes (Song et al. 2007), sedimentary structures, and grain size (Min et al. 2013). At each test point, flow velocity and water depth were measured. A Topcon GTS-102 N construction total station was used to collect data to detect the bedform (the detection of angle is achieved by 2 horizontal and 1 vertical measurement, and the measurement accuracy is $\pm(2 \text{ mm} + 2 \text{ ppm} \times D)$, where $\text{ppm} = 10^{-6}$ and D is measurement distance (km). The data processing for spatial analysis was performed using ArcGIS 10.0 software with the ordinary kriging interpolation technique and Gaussian Kernel Function (Merwade et al. 2006). Kennedy et al. (2008) indicated that a measurement density of about 0.05 points/m² of streambed was adequate to reduce the occurrence of error value to 10 % or less. In this study, the measurement density of streambed, erosional bank and depositional bank were roughly 0.007, 0.156 and 0.273, respectively. The modeling errors of interpolated contour maps for K_h were estimated to be 0.001 on the depositional stream bank and 0.008 on the erosional stream bank (Fig. 3). For streambed, two errors of K_v (0–30 cm) and Darcian flux were greater than 10 %, while another six errors were less than 1 % (Fig. 2). In general, the measurement density of the study site was considered relatively appropriate and achievable. Additionally, the temperatures of streambed sediments at two depths, 0 and 80 cm, were determined using a self-made pipe containing thermistors inside; the accuracy and response time were ± 0.05 °C and 15 min, respectively. The temperature was measured in the morning on two successive days, which was because winter temperature profiles were characterized by little or no temperature fluctuation in the surface water during the test period, and this approximates steady-state conditions (Gariglio et al. 2013). After completion of the K_v test, 45 sediment cores were collected from the streambed; however, considering the similarity of sediment texture within individual layers for the exposed streambed bank, only five cores were collected from the bank. All the sediment cores were sent to a laboratory for grain size analysis. After the samples were dried in the laboratory, the standard sieving method was used to separate them into 18 grain-size grades of which the finest sieve size was 0.025 mm and the coarsest one was 10 mm. Particles <0.075 mm were classified as silt and clay, particles of 0.075–2.0 mm as sand, and particles >2.0 mm as gravel.

Fig. 5 **a** Sediment cores collected from both exposed stream banks, and **b** on-site permeameter test to estimate the hydraulic conductivity of the sediment cores



Results and discussion

Heterogeneity of streambed K_v

The K_v values from the 75 measurements for the three connected layers cover three orders of magnitude and show a moderate degree of variability from 0.01 to 9.52 m/d (Table 1), which is within the range of K_v values reported in an earlier study in June 2014 (Jiang et al. 2015). The current test locations are close to those of the June 2014 study (with an average sediment thickness of 44.6 cm, see Fig. 6a). The non-parametric Kruskal-Wallis test is generally used to assess similarities in distribution between different populations of data

without assuming a normal distribution; thus, the similarities of K_v pairs and K_h pairs were estimated by the nonparametric Kruskal-Wallis test, and their probability (p) was calculated by MATLAB software. The difference is considered to be statistically significant when the p value was less than 0.05 (Dong et al. 2012). The result of a Kruskal-Wallis test between the data collected in June 2014 and January 2015 shows they belong to different populations ($p = 0.0028$). It has been found that the K_v values obtained in summer are larger and more variable than the K_v values determined in winter (Fig. 6a). Comparison with the applicable samples of this study indicates that the sediments are generally finer than they were in the former study (Jiang et al. 2015), which may be a result of

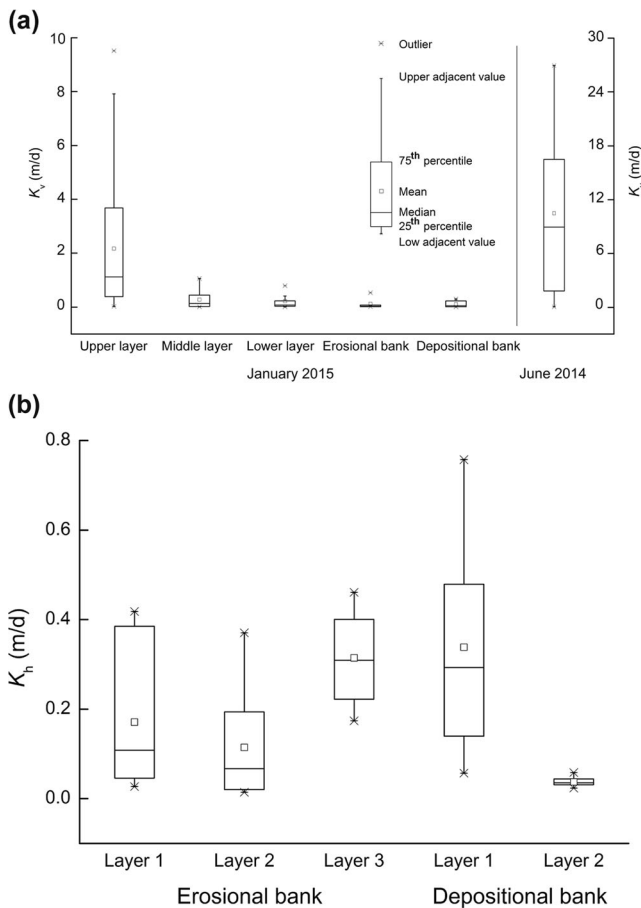


Fig. 6 Box plots of **a** K_v derived from the submerged streambed—January 2015 and June 2014 (the current test locations close to the previous ones with an average sediment thickness of 44.6 cm)—and both stream banks (January 2015), and **b** K_h for each layer on both banks (January 2015)

four factors. First, there was a flood in the interval between the tests, which likely deposited much fine sand, silt and clay, leading to a smaller K_v during and after the deposition process (Genereux et al. 2008; Chen 2011). Second, changing hydrologic conditions under which fine sediment could be carried downward and deposited by downwelling may have affected the K_v distribution (Song et al. 2007; Chen et al. 2013). The third factor is that the kinematic viscosity of water in winter is lower and affects the permeameter tests (K_v values increase by 1.8 % per 1 °C increase in water temperature), which may explain some of the variation (Dong et al. 2014). The fourth factor is that time-varying biological processes (clogging and declogging, bioturbation, and microbial gas production) can alter K_v (Kennedy et al. 2009; Dong et al. 2012).

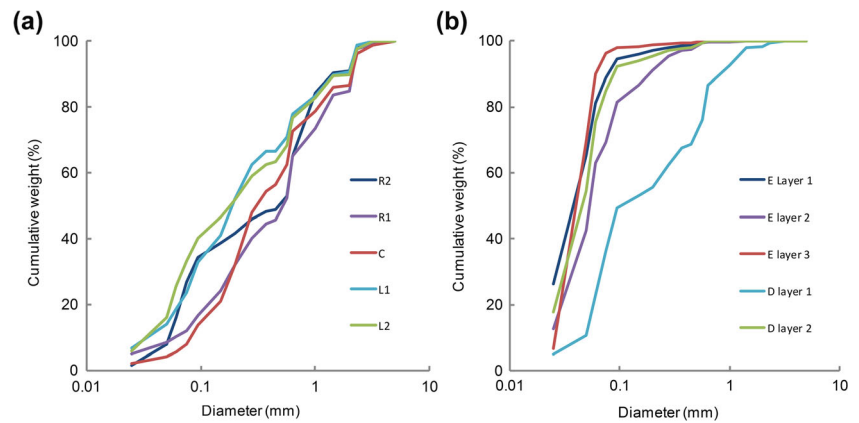
Generally, the K_v values differ greatly as a function of their position across the channel. The K_v distribution for the upper layer is generally highest at the center and towards the erosional bank (Fig. 2a) which has a larger grain size compared to the depositional bank (Fig. 7a). This result was consistent with previous studies (Genereux et al. 2008; Sebok et al. 2015; Wu

et al. 2016); however, this is not the case for the middle layer and lower layer (Fig. 2b,c). Leek et al. (2009) indicated no similar spatial pattern was found among different depth intervals, while Wu et al. (2016) found that a larger K_v for the upper layer more likely appeared in the center of the channel, but found different spatial patterns for the lower layers. Additionally, variability of K_v significantly differed between transects in an interval of 20 m. Along the flow direction, K_v values for the three layers are generally smallest in the middle of the stream reach sampled (Fig. 2a,b,c). K_v can change appreciably over transects of several meters (Genereux et al. 2008; Wu et al. 2016). Käser et al. (2009) showed that the mean value of hydraulic conductivity is smaller in the pool than in the riffle; however, in the upper layer, higher K_v values occur in the deepest area of the thalweg compared to its nearby test points (Fig. 2a).

A gradual decrease in the range, mean, and median K_v values occurred from the upper to the lower layer (Fig. 6a). The decreasing values of K with depth have been demonstrated by many researchers (Song et al. 2007; Min et al. 2013; Wu et al. 2016). The variability of K_v values was very similar for the middle layer and lower layer. According to the Kruskal-Wallis test results, the upper-layer/middle-layer values ($p = 0.0001$) and the upper-layer/lower-layer values ($p = 0.0001$) belong to different populations; however, differences between middle layer and lower layer were not significant statistically ($p = 1.0000$). An increase in extent of variation of K_v with depth occurred, though the K_v value decreased with depth (Ryan and Boufadel 2007; Wu et al. 2016). The values for the coefficient of variation (CV) for each layer were 1.17, 1.11 and 1.21 (Table 1), respectively. The results show that there was a relative high variability and CV for K_v in the upper layer. The lower layer has the highest CV value and contains the most silt and clay, which corresponds with the findings that the CV values are larger for silt/clay than for sand (Wu et al. 2016).

Spearman bivariate correlation analysis is used to verify whether two non-normally distributed variables are significantly correlated at the 95 % confidence level. The correlation coefficients of K_v to clay/silt (the average value of cumulative percentage in weight for particle size diameter <0.075 mm), median grain size (d_{50}), coefficient of uniformity (η), and sand (the average value of cumulative percentage in weight for particle size diameter from 0.075 mm to 2 mm) were -0.56 , 0.41 , -0.17 and 0.44 , respectively. The results for clay and silt ($n = 45$, $p = 0.000$), d_{50} ($n = 45$, $p = 0.006$), and sand ($n = 45$, $p = 0.002$) indicate that the correlation is significant at the 95 % confidence level. The differences in grain size distribution including sand, silt and clay, and d_{50} for the three layers could be a good indicator of decreased K_v with depth (Fig. 8; Table 1). A smaller percentage of silt/clay may have not influenced η , but

Fig. 7 Average grain-size distributions of upper layer sediments for **a** each location of the submerged streambed and **b** sediments for each layer on both stream banks (*E* erosional, *D* depositional)



it can result in a lower K_v value (Min et al. 2013). This could be the reason that the correlation between K_v and η was not significant ($n=45$, $p=0.277$). Sedimentary structure always plays an important role in influencing K_v (Leek et al. 2009). The sediment columns in the middle layer have a heterogeneous structure that results in smaller K_v values. Also, the small K_v values in the lower layer can be related to the compression from the overburden (Wu et al. 2016) and hyporheic processes (Song et al. 2007).

Heterogeneity of K_h and anisotropy on both stream banks

Different sedimentary features, at different elevations, were observed on both stream banks (Fig. 7b). On the erosional bank, layer 3 consisted of homogeneous silt with microlamination and layer 2 contained mainly silt and clay with no lamination or bedding (Table 2). Layer 1, on the depositional bank, contained a mixture of sand, silt, and clay, and layer 2 contained fine silt and clay (Table 2). This difference probably reflects a reduction in flow velocity during the deposition of each layer. Chen et al. (2014) investigated the sediment and measured K_h values of exposed streambed far away from the submerged streambed of the Weihe River (China); they also found the sediment varied from clay to medium sand from the upper to bottom layer.

All data for each layer are normally distributed (Table 2), but the range of K_h values are lower than the values of K_h in a high floodplain profile (Chen et al. 2014) and lower than exposed sediments in a floodplain (Cheng et al. 2013) of the Weihe River. This is because of the very fine sediment with no laminations and bedding. Six K_v values were determined for each bank, and the K_v values on both banks were generally lower than those in the streambed (Fig. 6a). This is not only related to the larger grain size of sediment in the streambed but also to more dynamic hydrologic conditions and biological processes there. Dong et al. (2012) showed K_v values were higher in a streambed than in exposed sediments in a point bar.

Generally, the spatial organization of K_h on both stream banks is significantly different. On the erosional bank, K_h values generally increased with elevation and layer 3 had a slightly larger value than the other two layers (Fig. 3a); however, the variation with elevation on the depositional bank was the opposite: the K_h values decrease with elevation—higher K_h values for layer 1 and smaller K_h values for layer 2 (Fig. 3b). The K_h values for each layer indicate that the depositional bank has a greater variability than the erosional bank (Fig. 6b, Table 2). Sebok et al. (2015) reported that the submerged streambed near a depositional bank displays the

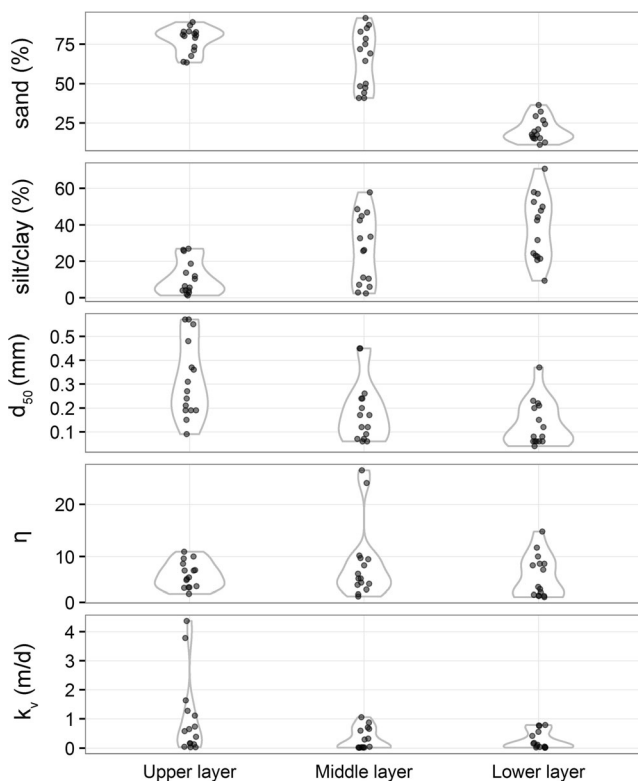


Fig. 8 Sediment grain-size distributions for the 45 samples collected from the three connected layers. Violin plots illustrate probability densities of the data number and values, and the d_{50} and η indicate values of median grain size and coefficient of uniformity, respectively

highest K_h values, while the thalweg close to the erosional bank is characterized by a lower K_h . Results of the Kruskal-Wallis test indicate that layer 3 and layer 2 ($p = 0.0235$), and layer 3 and layer 1 ($p = 0.0468$), on the erosional bank, belong to different populations. On the depositional bank, differences between layers were also statistically significant ($p = 0.0019$).

The anisotropic ratio (K_h/K_v) of both stream banks was determined at a total of 12 test locations (Table 2). The range for the banks varies from 0.7 to 6.0, including two values smaller than 1.0 and only one value larger than 4.0 (Fig. 9). It has been suggested that the anisotropic ratio of a stream bank is smaller than that of a submerged streambed, which is always larger than 4.0 (Chen 2004) and can be up to 50.0 (Sebok et al. 2015). The anisotropic ratio in exposed sediment was also investigated by Cheng et al. (2013), whose results showed that the anisotropic ratio was very close to 1.0, further illustrating that the anisotropic ratio is more variable and has the highest values on the depositional bank. This result was similar to the research results of Sebok et al. (2015) for a submerged streambed, which suggested higher anisotropic ratios appeared close to the depositional bank.

Vertical hydraulic gradient

Generally, the spatial distribution of VHGs has been found to range from upwelling to downwelling across lateral and longitudinal transects of the channel (Fig. 2d). It can be seen that most fluxes were upwelling and no exchange (VHG = 0) was found in this study. Downwelling flux appears near the depositional bank, which has smaller K_v values. Bank filtration processes coupled with downward flow in streambeds can concentrate fine sediments clogging streambeds (Schubert 2002); thus, smaller K_v values near the depositional bank may be the result of infiltration of fine sands. VHGs are relatively lower in the deepest area of the thalweg, and the highest VHGs appear near the depositional bank (Fig. 2d).

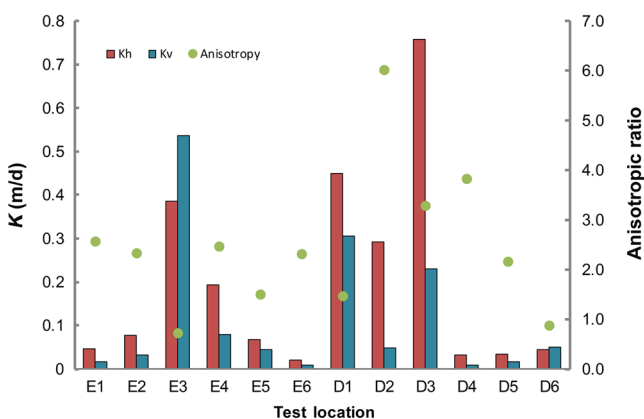


Fig. 9 Anisotropy (K_h/K_v) variations derived from 12 test locations on both stream banks. E1–E6 indicate test locations on the erosional bank and D1–D6 indicate the depositional bank

Specifically, the results illustrate that downwelling flux occurred in the deepest area and switched to upwelling flux in other areas, which could be a flux pattern in the thalweg which was induced by the change of streambed elevation (Fig. 2d,f). Downwelling and upwelling flow paths can be induced by streambed topography resulting from bedform and sinuosity at a small scale (Cardenas et al. 2004). It has been reported that downwelling paths were encountered where stream-water slope increased in the transition zone between pools and steeper channel units, after which upwelling paths occurred where stream-water slope decreased (Harvey and Bencala 1993).

The K_v distribution with depth and its heterogeneity can be related to VHGs. In fact, larger K_v values occur in the center towards the erosional bank where generally there is upwelling. Similar results were reported by Datry et al. (2015), which indicated K was higher in upwelling areas as compared to downwelling areas. Mostly upwelling flux corresponds with the result that K_v has a decreasing trend from upper layer to lower layer. Chen et al. (2013) confirmed that, in gaining stream reaches, hydraulic conductivity decreases with depth; additionally, VHG values vary from -0.19 to 0.18 and exhibit an inverse distribution to K_v values (Fig. 2a,e). Relatively larger VHGs tend to be induced in lower K areas because the homogeneity of groundwater discharge appears to be maintained by the permeability distribution of the streambed (Käser et al. 2009; Kennedy et al. 2009; Sebok et al. 2015).

Spatial variability of Darcian flux and temperature variations of the streambed

Spatial variability of Darcian flux was highly variable in space, ranging from -380 to 336 mm/d (Fig. 2e), which is within the range of specific discharge determined by VHGs in several former studies (Chen et al. 2009; Käser et al. 2009; Kennedy et al. 2010). One of the clearest aspects of spatial variability was lateral variability across the channel. This distribution of Darcian flux was focused near the erosional bank that contains mostly sand with large K_v values and is in contrast to the relatively smaller values that appear near the depositional bank with lower K_v values (Fig. 10). Streambed heterogeneity of K_v distribution and bedforms are major controlling factors in hyporheic water exchange (Cardenas et al. 2004).

In this study, Darcian fluxes were highly variable. Käser et al. (2009) suggested VHGs would be misleading indicators of the intensity of flow because the actual fluxes can be relatively homogeneous despite a high variability in VHGs. However, a rapidly increasing number of studies have demonstrated that heat can be used as a tracer that reflects hyporheic water exchange (Conant 2004; Schmidt et al. 2007; Hatch et al. 2010; Anibas et al. 2011); therefore, the temperature was determined at the depths of 0 cm (stream

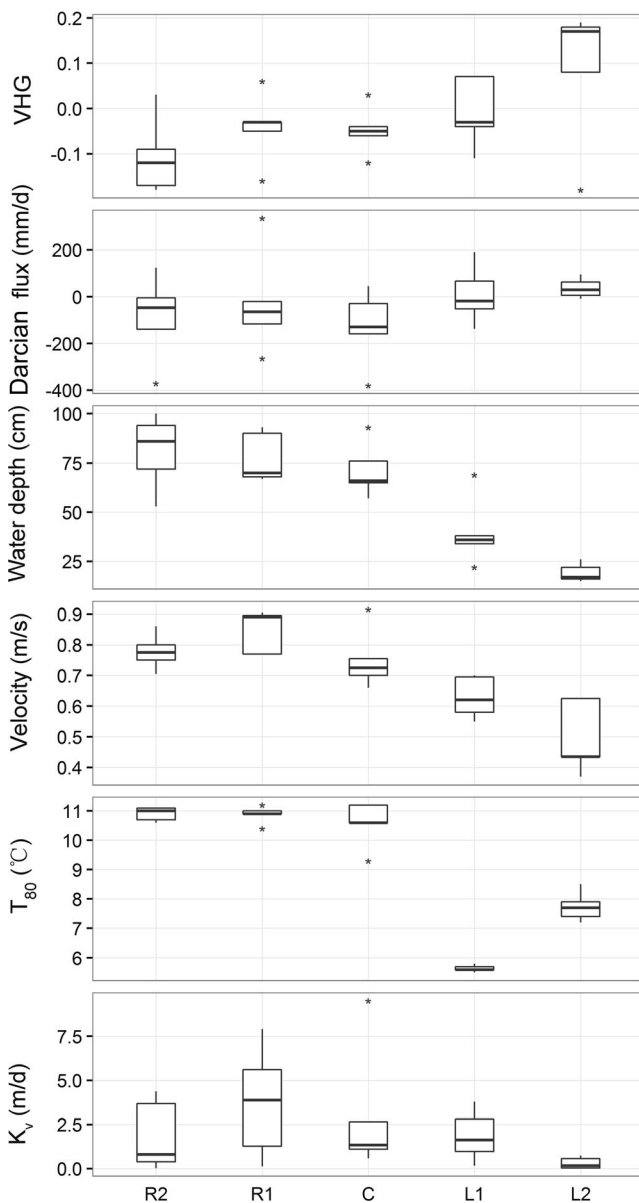


Fig. 10 Box plot of hydrologic attributes for each test location of the submerged streambed. T_{80} indicates the sediment temperature at the depth of 80 cm

water and sediments interface) and 80 cm of streambed sediments during the measurement of VHGs.

The temperature distribution at a depth of 80 cm of sediment had values in the range of 7.2 to 11.2 °C with an average of 9.9 °C with obvious lateral variability (Fig. 2g). The highest temperature values were near the erosional bank and generally showed a decreasing trend towards the depositional bank (Fig. 10). Conant (2004) demonstrated high discharge locations were associated with relatively warm areas of the streambed in winter. Temperature profiles from streambed sediments to groundwater have been considered to reflect the extent of discharge through the streambed (Schmidt et al. 2007; Anibas et al. 2011). Temperature gradients were determined for the

stream water and sediment interface (0 cm) and streambed sediment (80 cm); the variation of temperature gradient was generally similar to temperature distributions at a depth of 80 cm (Fig. 2g,h). The temperature gradient difference in each location of the channel can be compared to the magnitude of Darcian flux distribution (Schmidt et al. 2007). The temperature gradients at the deepest area of the thalweg were lower than at other test points near the erosional bank, suggesting that the high pressure head in the deepest area of the thalweg probably hindered the conductance of heat from groundwater fluxes through lower streambed sediments up to the surface (0 cm) streambed sediments. Kennedy et al. (2010) indicated Darcian flux determined using the VHG method and seepage meter method had the same direction, and the two methods gave similar spatial patterns of groundwater seepage rates as well, suggesting that the Darcian flux distribution in this study is dependable.

Conclusions

This report not only elucidates the quantitative relations between streambed K_v , VHG, Darcian flux determined by VHGs, temperature, stream geomorphology and bedforms in the studied streambed, but it also describes the heterogeneity and anisotropy of its adjacent two stream banks. In anabranching channels, streambed attributes of K_v for three connected layers, and their VHGs, were determined using an in-situ permeameter test method. An on-site permeameter test method was used to determine the K_h and anisotropy of both its associated stream banks. The conclusions from this study can be summarized as elucidated in the following.

In general, all hydrologic attributes showed high spatial variability. In the submerged streambed, a gradual decrease in K_v values with depth was observed, but higher values of K_v occurred around the center or close to erosional banks. Compared to exposed stream banks, K_v values were generally higher in the submerged streambed. With an increase of elevation to stream stage, K_h values increased on the erosional bank while they decreased on the depositional bank. The variation extent of anisotropic ratio (K_h/K_v) was higher on the depositional bank than those on the erosional bank; furthermore, spatial distribution of VHGs indicates that downwelling flux occurred in the deepest area, while upwelling flux appeared in the other area along the thalweg, which might result from the change of streambed elevation. Near the erosional bank, the value of the Darcian flux in the submerged streambed was higher. This study deepens understanding of heterogeneity of hydraulic conductivity and Darcian flux and provides scientific reference for more appropriate modeling approaches of stream–aquifer interactions.

Streambed surface sediments are always dynamic and highly variable; more work is needed to assess streambed

hydraulic conductivity and Darcian flux. Further research will be devoted to more approaches which combine the VHGs, heat, seepage metering and modeling to determine specific discharge across a variety of natural stream morphologies and microtopography.

Acknowledgements This study was supported by the National Natural Science Foundation of China (Grant Nos. 51379175 and 51079123), Specialized Research Fund for the Doctoral Program of Higher Education (Grant No. 20136101110001), Program for Key Science and Technology Innovation Team in Shaanxi Province (Grant No. 2014KCT-27), the Hundred Talents Project of the Chinese Academy of Sciences (Grant No. A315021406), and the Program for Graduated Student Innovation Talents Training in Northwest University (Grant No. YZZ14011). Jiaxuan Li, Xiaogang Yang, and Junlong Zhang provided help with field work and technical support. We are especially grateful to the editor, associate editor, and two anonymous reviewers for their helpful suggestions, which improved the quality of the manuscript.

References

- Anibas C, Buis K, Verhoeven R, Meire P, Batelaan O (2011) A simple thermal mapping method for seasonal spatial patterns of groundwater–surface water interaction. *J Hydrol* 397(1):93–104. doi:10.1016/j.jhydrol.2010.11.036
- Battle-Aguilar J, Xie YQ, Cook PG (2015) Importance of stream infiltration data for modelling surface water–groundwater interactions. *J Hydrol* 528:683–693
- Boano F, Camporeale C, Revelli R, Ridolfi L (2006) Sinuosity-driven hyporheic exchange in meandering rivers. *Geophys Res Lett* 33(18). doi: 10.1029/2006GL027630
- Böhlke JK, O’Connell ME, Prestegard KL (2007) Ground water stratification and delivery of nitrate to an incised stream under varying flow conditions. *J Environ Qual* 36(3):664–680. doi:10.2134/jeq2006.0084
- Boulton AJ, Findlay S, Marmonier P, Stanley EH, Valett HM (1998) The functional significance of the hyporheic zone in streams and rivers. *Annu Rev Ecol Syst* 29:59–81
- Brunke M, Gonser T (1997) The ecological significance of exchange processes between rivers and groundwater. *Freshw Biol* 37(1):1–33
- Cardenas MB (2009) Stream–aquifer interactions and hyporheic exchange in gaining and losing sinuous streams. *Water Resour Res* 45(6). doi:10.1029/2008WR007651
- Cardenas MB, Wilson JL, Zlotnik VA (2004) Impact of heterogeneity, bed forms, and stream curvature on subchannel hyporheic exchange. *Water Resour Res* 40(8). doi:10.1029/2004WR003008
- Chen XH (2004) Streambed hydraulic conductivity for rivers in south-central Nebraska. *J Am Water Resour Assoc* 40(3):561–574. doi:10.1111/j.1752-1688.2004.tb04443.x
- Chen XH (2011) Depth-dependent hydraulic conductivity distribution patterns of a streambed. *Hydrol Process* 25:278–287. doi:10.1002/hyp.7844
- Chen XH, Yin YF (1999) Evaluation of streamflow depletion for vertical anisotropic aquifers. *J Environ Syst* 27(1):55–70
- Chen XH, Song JX, Cheng C, Wang DM, Lackey SO (2009) A new method for mapping variability in vertical seepage flux in streambeds. *Hydrogeol J* 17(3):519–525. doi:10.1007/s10040-008-0384-0
- Chen XH, Dong WH, Ou GX, Wang ZW, Liu C (2013) Gaining and losing stream reaches have opposite hydraulic conductivity distribution patterns. *Hydrol Earth Syst Sci* 10:1693–1723. doi:10.5194/hessd-10-1693-2013
- Chen XH, Mi HC, He HM, Liu RC, Gao M, Huo AD, Cheng DH (2014) Hydraulic conductivity variation within and between layers of a high floodplain profile. *J Hydrol* 515:147–155. doi:10.1016/j.jhydrol.2014.04.052
- Cheng DH, Chen XH, Huo AD, Gao M, Wang WK (2013) Influence of bedding orientation on the anisotropy of hydraulic conductivity in a well-sorted fluvial sediment. *Int J Sediment Res* 28(1):118–125. doi:10.1016/S1001-6279(13)60024-4
- Conant B (2004) Delineating and quantifying ground water discharge zones using streambed temperatures. *Groundwater* 42(2):243–257
- Datry T, Lamouroux N, Thivin G, Descloux S, Baudoin JM (2015) Estimation of sediment hydraulic conductivity in river reaches and its potential use to evaluate streambed clogging. *River Res Appl* 31(7):880–891. doi:10.1002/rra.2784
- Dong WH, Chen XH, Wang ZW, Ou GX, Liu C (2012) Comparison of vertical hydraulic conductivity in a streambed-point bar system of a gaining stream. *J Hydrol* 450:9–16. doi:10.1016/j.jhydrol.2012.05.037
- Dong WH, Ou GX, Chen XH, Wang ZW (2014) Effect of temperature on streambed vertical hydraulic conductivity. *Hydrol Res* 45(1):89–98
- Freeze AR, Cherry JA (1979) *Groundwater*. Prentice-Hall, Upper Saddle River, NJ
- Gariglio FP, Tonina D, Luce CH (2013) Spatiotemporal variability of hyporheic exchange through a pool-riffle-pool sequence. *Water Resour Res* 49(11):7185–7204. doi:10.1002/wrcr.20419
- Genereux DP, Leahy S, Mitasova H, Kennedy CD, Corbett DR (2008) Spatial and temporal variability of streambed hydraulic conductivity in West Bear Creek, North Carolina, USA. *J Hydrol* 358(3–4):332–353. doi:10.1016/j.jhydrol.2008.06.017
- Gomez-Velez JD, Krause S, Wilson JL (2014) Effect of low-permeability layers on spatial patterns of hyporheic exchange and groundwater upwelling. *Water Resour Res* 50(6):5196–5215. doi:10.1002/2013WR015054
- Harvey JW, Bencala KE (1993) The effect of streambed topography on surface–subsurface water exchange in mountain catchments. *Water Resour Res* 29(1):89–98
- Hatch CE, Fisher AT, Ruehl CR, Stemler G (2010) Spatial and temporal variations in streambed hydraulic conductivity quantified with time-series thermal methods. *J Hydrol* 389(3–4):276–288. doi:10.1016/j.jhydrol.2010.05.046
- Huang HQ, Nanson GC (2007) Why some alluvial rivers develop an anabranching pattern. *Water Resour Res* 43(7). doi: 10.1029/2006WR005223
- Hvorslev MJ (1951) Time lag and soil permeability in ground-water observations. *US Army Bull* 36, Waterways Experiment Station, US Army Corps of Engineers, Vicksburg, MI, 50 pp
- Jiang WW, Song JX, Zhang JL, Wang YY, Zhang N, Zhang XH, Long YQ, Li JX, Yang XG (2015) Spatial variability of streambed vertical hydraulic conductivity and its relation to distinctive stream morphologies in the Beiluo River, Shaanxi Province, China. *Hydrogeol J* 23(7):1617–1626. doi:10.1007/s10040-015-1288-4
- Käser DH, Binley A, Heathwaite AL, Krause S (2009) Spatio-temporal variations of hyporheic flow in a riffle-step-pool sequence. *Hydrol Process* 23(15):2138–2149. doi:10.1002/hyp.7317
- Kennedy CD, Genereux DP, Mitasova H, Corbett DR, Leahy S (2008) Effect of sampling density and design on estimation of streambed attributes. *J Hydrol* 355(1):164–180. doi:10.1016/j.jhydrol.2008.03.018
- Kennedy CD, Genereux DP, Corbett DR, Mitasova H (2009) Spatial and temporal dynamics of coupled groundwater and nitrogen fluxes through a streambed in an agricultural watershed. *Water Resour Res* 45(9). doi: 10.1029/2008WR007397
- Kennedy CD, Murdoch LC, Genereux DP, Corbett DR, Stone K, Pham P, Mitasova H (2010) Comparison of Darcian flux calculations and seepage meter measurements in a sandy streambed in North

- Carolina, United States. *Water Resour Res* 46(9). doi:10.1029/2009WR008342
- Koch JC, McKnight DM, Neupauer RM (2011) Simulating unsteady flow, anabranching, and hyporheic dynamics in a glacial meltwater stream using a coupled surface water routing and groundwater flow model. *Water Resour Res* 47(5). doi:10.1029/2010WR009508
- Leek R, Wu JQ, Wang L, Hanrahan TP, Barber ME, Qiu HX (2009) Heterogeneous characteristics of streambed saturated hydraulic conductivity of the Touchet River, south eastern Washington, USA. *Hydrol Process* 23(8):1236–1246. doi:10.1002/hyp.7258
- Levy J, Birck MD, Mutiti S, Kilroy KC, Windeler B, Idris O, Allen LN (2011) The impact of storm events on a riverbed system and its hydraulic conductivity at a site of induced infiltration. *J Environ Manag* 92:1960–1971. doi:10.1016/j.jenvman.2011.03.017
- Malard F, Tockner K, Dole-Olivier MJ, Ward JV (2002) A landscape perspective of surface–subsurface hydrological exchanges in river corridors. *Freshwater Biol* 47(4):621–640
- Merwade VM, Maidment DR, Goff JA (2006) Anisotropic considerations while interpolating river channel bathymetry. *J Hydrol* 331(3):731–741. doi:10.1016/j.jhydrol.2006.06.018
- Min LL, Yu JJ, Liu CM, Zhu JT, Wang P (2013) The spatial variability of streambed vertical hydraulic conductivity in an intermittent river, northwestern China. *Environ Earth Sci* 69:873–883. doi:10.1007/s12665-012-1973-8
- Pryshlak TT, Sawyer AH, Stonedahl SH, Soltanian MR (2015) Multiscale hyporheic exchange through strongly heterogeneous sediments. *Water Resour Res* 51(11):9127–9140
- Ryan RJ, Boufadel MC (2007) Evaluation of streambed hydraulic conductivity heterogeneity in an urban watershed. *Stochastic Environ Res Risk Assess* 21(4):309–316. doi:10.1007/s00477-006-0066-1
- Sawyer AH, Cardenas MB (2009) Hyporheic flow and residence time distributions in heterogeneous cross-bedded sediment. *Water Resour Res* 45(8). doi:10.1029/2008WR007632
- Schmidt C, Conant B, Bayer-Raich M, Schirmer M (2007) Evaluation and field-scale application of an analytical method to quantify groundwater discharge using mapped streambed temperatures. *J Hydrol* 347(3):292–307. doi:10.1016/j.jhydrol.2007.08.022
- Schubert J (2002) Hydraulic aspects of riverbank filtration: field studies. *J Hydrol* 266(3):145–161
- Sebok E, Duque C, Engesgaard P, Boegh E (2015) Spatial variability in streambed hydraulic conductivity of contrasting stream morphologies: channel bend and straight channel. *Hydrol Process* 29(3):458–472. doi:10.1002/hyp.10170
- Shope CL, Constantz JE, Cooper CA, Reeves DM, Pohl G, McKay WA (2012) Influence of a large fluvial island, streambed, and stream bank on surface water–groundwater fluxes and water table dynamics. *Water Resour Res* 48(6). doi:10.1029/2011WR011564
- Song JX, Chen XH, Cheng C, Summerside S, Wen FJ (2007) Effects of hyporheic processes on streambed vertical hydraulic conductivity in three rivers of Nebraska. *Geophys Res Lett* 34. doi: 10.1029/2007GL029254
- Song JX, Chen XH, Cheng C, Wang DM, Lackey S, Xu ZX (2009) Feasibility of grain-size analysis methods for determination of vertical hydraulic conductivity of streambeds. *J Hydrol* 375(3–4):428–437. doi:10.1016/j.jhydrol.2009.06.043
- Wu GD, Shu LC, Lu CP, Chen XH (2016) The heterogeneity of 3-D vertical hydraulic conductivity in a streambed. *Hydrol Res* 47(1):15–26. doi:10.2166/nh.2015.224
- Xi HY, Zhang L, Feng Q, Si JH, Chang ZQ, Yu TF, Li JG (2015) The spatial heterogeneity of riverbed saturated permeability coefficient in the lower reaches of the Heihe River Basin, Northwest China. *Hydrol Process* 29(23):4891–4907. doi:10.1002/hyp.10544